High-resolution spatiotemporal forecasting of the European crane migration

K. De Koning [a,*], L. Nilsson [b], J. Månsson [b], O. Ovaskainen [c,d], B. Kranstauber [e], M. Arp [f], J.K. Schakel [f]

[a] *Earth Systems and Global Change group, Wageningen University, P.O. Box 9101, 6700HB Wageningen, The Netherlands*
[b] *Grimsö Wildlife Research Station, Department of Ecology, Swedish University of Agricultural Sciences, Riddarhyttan, Sweden*
[c] *Department of Biological and Environmental Science, University of Jyväskylä, P.O. Box 35 (Survontie 9C), FI-40014 Jyväskylä, Finland*
[d] *Organismal and Evolutionary Biology Research Programme, Faculty of Biological and Environmental Sciences, University of Helsinki, P.O. Box 65, Helsinki 00014, Finland*
[e] *Institute for Biodiversity and Ecosystem Dynamics, University of Amsterdam, Amsterdam, The Netherlands*
[f] *Sensing Clues Foundation, Amsterdam, Netherlands*

ARTICLE INFO

ABSTRACT

In this paper we present three different models to forecast bird migration. They are species-specific individual-based models that operate on a high spatiotemporal resolution (kilometres, 15 min-hours), as an addition to radar-based migration forecast models that currently exist. The models vary in complexity, and use GPS-tracked location, flying direction and speed, and/or wind data to forecast migration speed and direction. Our aim is to quantitatively evaluate the forecasting performance and assess which metrics improve forecasts at different ranges. We test the models through cross-validation using GPS tracks of common cranes during spring and autumn migration. Our results show that recordings of flight speed and direction improve the accuracy of forecasts on the short range (<2 h). Adding wind data at flight altitude results in consistent improvements of the forecasts across the entire range, particularly in the predicted speed. Direction forecasts are less affected by adding wind data because cranes mostly compensate for wind drift during migration. Migration in spring is more difficult to forecast than in autumn, resulting in larger errors in flight speed and direction during spring. We further find that a combination of flight behaviours – thermal soaring, gliding, and flapping – complicates the forecasts by inducing variance in flight speed and direction. Fitting those behaviours into flight optimisation models proves to be challenging, and even results in significant biases in speed forecasts in spring. We conclude that flight speed is the most difficult parameter to forecast, whereas flight direction is the most critical for practical applications of these models. Such applications could e.g., be prevention of bird strikes in aviation or with wind turbines, and public engagement with bird migration.

1. Introduction

Contemporary anthropogenic pressures on ecosystems bring rapid changes beyond the historic realm. Hence, conservationists are challenged to identify and act promptly to undesirable changes to ecosystems. In ecological modelling this means that we need to focus on near-term forecasting (Clark et al., 2001; Dietze et al. 2018; Lewis et al. 2023) in order to capture ecosystem trends in current time and to provide quantitative support for decision making in conservation. Forecasting ecosystem changes requires synthesising the state-of-the-art of ecological knowledge and process-based models, and testing these against new data. The increased volume of automated data collection and sharing (Arts et al. 2015; van der Wal and Arts 2015; Keitt and Abelson 2021) provides an important opportunity for testing and updating of model forecasts (de Koning et al. 2023). Effectively, near-term forecasts can provide timely quantitative insights in the uncertainty of model predictions and inaccuracies.

Ecological forecasting is already fairly common in bird migration (Bouten et al. 2005; Fisher et al. 2012; Horton et al. 2021; van Belle et al. 2007; Van Doren and Horton 2018), due to the extensive variability and uncertainty in spatio-temporal scale, but also due to broad public interest. Bird migrations are well-studied and they respond predictably to

well-monitored environmental drivers such as weather, making bird migration an ideal phenomenon to forecast. Bird migration forecasts are particularly useful for the legal protection of important migration corridors (Bradarić 2022; Van Doren and Horton 2018; Horton et al. 2021; Kranstauber et al. 2022; Lippert et al. 2022), for example to avoid wind turbine collisions or light pollution, or for aviation safety (van Belle et al. 2007; van Gasteren et al. 2019; Holleman 2008; Ruhe 2008). However, current applications focus primarily on large scale patterns, forecasting migration intensity in metrics such as expected spatial distribution of birds over several hours or days using resolutions of up to several hundred square kilometres. The models are typically trained on radar data and therefore generate forecasts of expected reflectivity values around specific radar sites. Hence, they cannot be used to track individual flocks of migratory birds over continuous space. In fact, the majority of these models do not distinguish between bird species, despite that species have vastly different migration traits and body sizes, with relevant consequences for the risk posed on birds and humans (Metz et al. 2020).

We therefore stress the need for species specific forecasts that focus on individual flocks in addition to large-scale radar-based forecasts. Some examples of studies that apply the so-called agent-based or individual-based approach to model the migration of individuals or flocks of birds are on wheatears (*Oenanthe oenanthe*) (Bulte et al. 2014), white storks (*Ciconia ciconia*) (van Loon 2011; Oloo et al. 2018), on bird migration over mountainous terrain (Aurbach et al. 2018), and on nocturnal migration of passerines (McLaren et al. 2012). These models ultimately focus on emerging patterns and behavioural traits in migration such as departure decisions (Duriez et al. 2009) and migration routes (Aurbach et al. 2018), and are less concerned with individual animal movement. Moreover, the aforementioned individual-based models (IBMs) of bird migration are used for understanding migration dynamics and exploring what drives these dynamics on a population level, not for forecasting migrations of individual birds. Whereas in fact the individual-based approach in principle allows you to do both: tracking individual flocks and emerging patterns on the population level. IBMs are however seldomly used for forecasting, but see Randon et al. (2022) who use state-space models to predict movements of killer whale (*Orcinus orca*) pods.

In this study, we demonstrate the first application of individual-based forecasting in bird migration, and quantitatively assess the forecasting limits (i.e., errors, biases and forecast horizon) of three different models that deal with migration forecasts. The three models increase in complexity and required data for parameterisation. We compare their forecasting performance over various temporal ranges and evaluate the implications for developing individual-based bird migration forecasts focusing on individual species and individual flocks by performing cross-validation on GPS tracks of tagged individuals. Moreover, we illustrate the ecological knowledge and data required for such forecasts, and show that the process of building a migration forecast model may also reveal new insights in bird migration ecology. The common crane (*Grus grus*), an iconic species that uses a combination of soaring and powered flight during migration, was used as a model species to forecast daily migration patterns (migration speed, flight direction) over the Netherlands, Belgium, Luxemburg and parts of France and Germany. In contrast to statistically-inferred state-space models that often make use of high-frequency observation data (e.g., telemetry data), our aim is to explore the forecasting potential of mechanistic migration models that are more flexible in their data requirement and in the frequency of observations. The models applied in the present study can also be applied to ground observation data from birdwatchers, which allows tracking a large number of individuals - not just those equipped with GPS tags - covering the complete width of the common crane's West European migration flyway. Applications of timely and precise migration forecast can provide for example early warning systems and selective stopping of wind turbines to prevent collisions (de Lucas et al. 2012), cost-effective land management and protection along the crane migration routes (Horton et al. 2021), and public engagement with the crane migration

by providing useful data and increasing the likelihood of observing cranes from the ground[1].[2]

2. Methods

2.1. Study area and data

2.1.1. GPS tracks

Crane GPS location data was derived from individuals captured during the period July 2016 until July 2020 (Table 1). A total of 25 juvenile common cranes were captured and tagged with legmount ($N = 24$) and backpack transmitters ($n = 1$) in south-central Sweden 2016–2020 (59–60° N and 15–16° E; Ornitela models OT-L40–2GC, OT-L40–3GC, OT-R193 G), see Månsson et al. (2013) for details about the area. The cranes were hand-captured using a short-distance run from a car or a hide. The cranes were marked between 25 June and 27 July at an approximate age of 6–8 weeks. The individuals weighed 2150–4200 gs at the time of tagging. The family groups normally split at the wintering grounds in January (Alonso et al. 1984), and we thus assume that each juvenile was accompanied by the parental pair and occasionally by one sibling during the first autumn migration study period. All captures and tagging fulfilled ethical requirements for research on wild animals after approval from the Animal Ethics Committee of central Sweden (5.2.18–2830/16 and 5.8.18–09,841/2022).

The dataset contains tracks of autumn migration from 2016 to 2021, and spring migration from 2017 to 2021 with a temporal resolution of 15 min (Fig. 1). The dataset is filtered to contain only migration days, by selecting days where cranes moved at least 100 km. I.e.: the geodesic distance between the first and the last GPS fix that day is >100 km.[3] Within these migration days we filtered the GPS fixes that fall within our study area of the Benelux, part of northern France and northwest Germany (latitude=49–54° north, longitude=1–9° east) (see blue box Fig. 1). Next, we classified the GPS fixes on migration days into '*resting*' and '*flying*' based on speed between two fixes and assigned it to the latter fix, with a cut-off value of 10 km per hour (relative to ground). This cut-off value is initially chosen manually based on a visual inspection of a histogram of ground speeds and subsequently cross-checked by fitting a bi-modal distribution, which highlights two distinct distributions for resting and flying cranes (Appendix II). There is some overlap in ground speed distributions between flying and resting cranes, which is likely caused by combined flying and resting behaviour in the 15-minute time interval between two GPS fixes. We acknowledge that hidden Markov models may provide a more solid and accurate behaviour classification (Michelot et al. 2016). Yet, given the clear visual discrepancy between the two probability distributions, and the relatively small number of observations with 'hybrid' behaviour, we decided that this simplified procedure would suffice for our further analysis. In our further analysis of migration movement metrics (section 2.2.2 and 2.2.3) we included all GPS fixes on migration days that are classified as *flying*.

2.1.2. Weather data

We used hourly weather reanalysis data from ECMWF ERA5[4] (Hersbach et al. 2023) on pressure levels 950hPa and 975hPa to analyse the wind effect on flight patterns (section 2.2.2 and 2.2.3). We downloaded the u-component and v-component of wind (metres per second) at 950hPa and 975hPa on all migration days for our study area

---

Table 1
Summary of the captured individuals included in this study.

| Individual id	Capture date	Weight when captured (g)	Number of fixes	Number of autumn migration cycles	Number of spring migration cycles	Type of transmitters
16,077	05/07/2016	3800	112	4	3	leg mounted
16,078	05/07/2016	NA	12	1	1	leg mounted
16,079	06/07/2016	3950	8	1	0	backpack
17,461	27/07/2017	3000	64	0	1	leg mounted
17,462	05/07/2017	3000	54	0	2	leg mounted
17,463	30/06/2017	2350	109	2	1	leg mounted
17,464	30/06/2017	3750	98	2	1	leg mounted
17,466	30/06/2017	4050	110	2	2	leg mounted
17,467	03/07/2017	2900	137	4	3	leg mounted
17,467	03/07/2017	2900	123	2	2	leg mounted
180,863	11/07/2018	3300	104	2	2	leg mounted
180,864	04/07/2018	2800	81	2	1	leg mounted
180,865	11/07/2018	2150	164	3	2	leg mounted
180,866	11/07/2018	3000	206	3	3	leg mounted
180,867	04/07/2018	2600	162	3	2	leg mounted
191,854	08/07/2019	4200	68	1	2	leg mounted
191,855	27/06/2019	2950	103	2	1	leg mounted
191,856	03/07/2019	3250	147	3	2	leg mounted
191,857	09/07/2019	3450	55	1	1	leg mounted
191,858	09/07/2019	2950	98	3	2	leg mounted
191,859	25/06/2019	3300	38	1	0	leg mounted
201,845	30/06/2020	3100	124	2	1	leg mounted
201,846	03/07/2020	3100	32	1	1	leg mounted
201,847	30/06/2020	3100	51	2	1	leg mounted
201,848	03/07/2020	2250	71	2	0	leg mounted
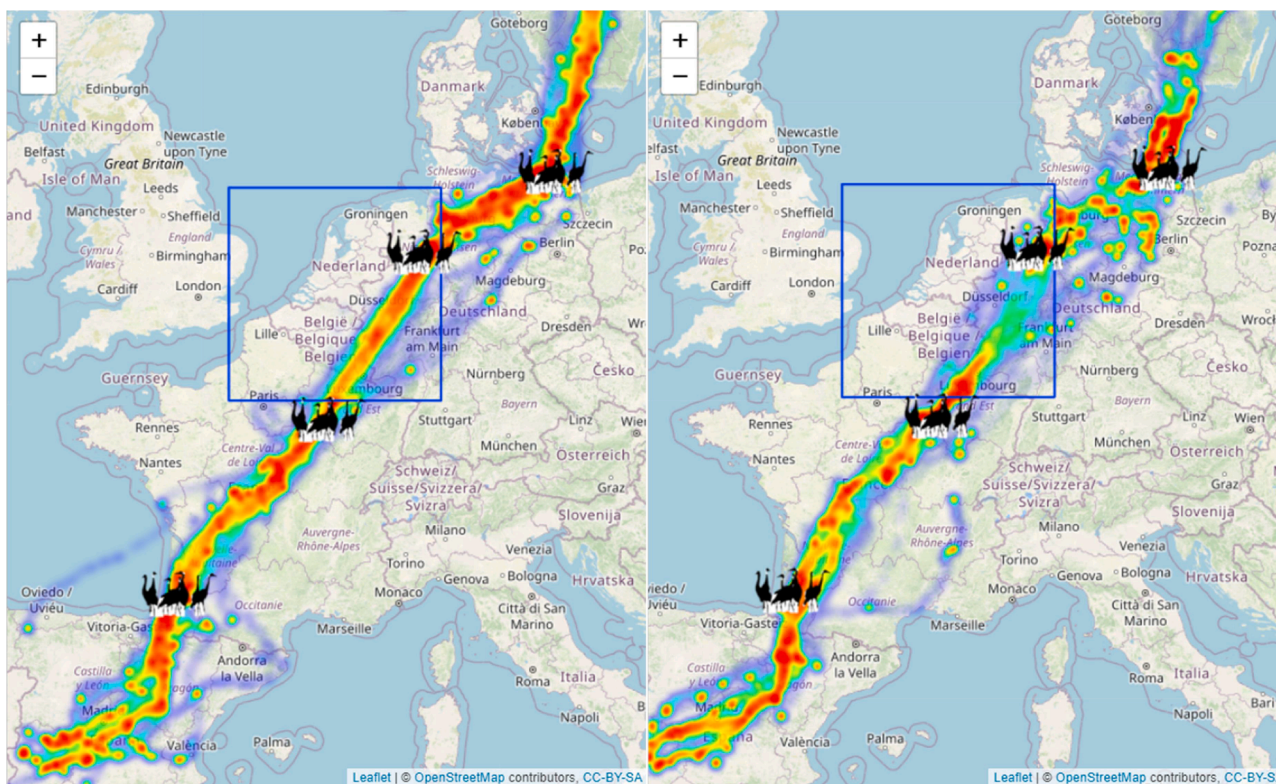
Fig. 1. The migration route of the GPS-tagged common cranes during autumn migration (left) and spring migration (right). The crane icons indicate important stopover sites along the route. The blue box indicates the bounds of our study area.

(48.875N–54.125 N, 0.875E–9.125E), and extracted the wind data for each GPS fix classified as *flying* (Section 2.1.1) based on location, altitude and time stamp. Time stamp was rounded off two whole hours and matched with the corresponding ERA5 wind map. We converted altitude to an estimated pressure at that altitude using an online conversion tool based on International Standard Atmosphere (ISO 2533:1975), and attributed the 975hPa maps to GPS fixes above 967.5hPa and the

950hPa maps to GPS fixes below 967.5hPa, where the majority of flying occurs.

2.2. Model specification

We constructed three models (M1, M2 and M3) to forecast crane migration. More specifically, these models predict the location of a

flying crane after time Δt since its last observation at a location (x_0, y_0). We consider a discrete-time model that runs at the intervals of 900 s (15 min), to match the temporal resolution at which we analyse the GPS data. We denote the time intervals by $i = 0, 1, 2, \ldots$, where $i = 0$ corresponds to the last observed location and the model predictions are made for times $\Delta t = 900i$. The models are parameterized in terms of speed and direction during flight. The models M1 and M2 utilize GPS data only, whereas model M3 utilize weather data as well (Table 2). We next describe the models, then describe how their parameters were estimated from the data, and finally how we evaluated the predictive performance of the models through cross-validation.

The baseline model M1 assumes constant speed and fixed direction towards the target. We denote by $\overrightarrow{V_{ground}}$ the velocity vector of the crane with respect to ground, by $v = |\overrightarrow{V_{ground}}|$ its magnitude and hence the speed, and by $\overrightarrow{D_{ground}} = \overrightarrow{V_{ground}}/v$ the unit vector of its direction. We assume that, given the current location (x, y), the direction is towards a known target: Lac du Der (48.58 N, 4.76E) in autumn and Hemelsmoor (53.24 N, 9.22E) in spring. The predicted location after time $\Delta t = 900i$ is calculated deterministically as $(x_i, y_i) = (x_0, y_0) + \Delta t v \overrightarrow{D_{ground}}$, and the parameter vector θ of this model contains only the speed parameter: $\theta = (v)$.

The model M2 allows for variation in both the speed and direction by assuming that they are different for each 15 min interval. We assume that these vary in a temporally autocorrelated manner, modelling primarily the effect of wind that we will incorporate explicitly in model M3. We denote by v_i the speed for time interval i (from time point i to $i+1$) and by $\vartheta_0 - \vartheta_{target,i}$ the angle between ground direction and target direction. Denoting the speed at time of the observation (and hence also for the first 15 min interval) by v_0, we assume that the speed converges towards its mean v_μ as

$$v_i = v_\mu + (v_0 - v_\mu)\gamma_v^i, \tag{1}$$

where γ_v models the temporal autocorrelation in flight speed over the 15 min interval. Similarly, denoting the direction (in degrees, ranging from 0 to 360, where 0 equals north) at time of the observation by ϑ_0, we assume that the direction converges towards the target direction ϑ_{target} as

$$\vartheta_i = \vartheta_{target,i} + (\vartheta_0 - \vartheta_{target,i})\gamma_\vartheta^i, \tag{2}$$

where γ_ϑ models the temporal autocorrelation in direction. Note that here we have included the index of the time step i to the target direction, because that changes depending on to where the crane has been predicted to move since the time of the observation. The parameter vector θ of this model is $\theta = (v_\mu, \gamma_v, \gamma_\vartheta)$.

The model M3 also assumes that speed and direction vary but models them as a function of weather data. We denote the x- and y- components of wind for interval i by $w_{x,i}$ and $w_{y,i}$, and the x- and y- components of air speed by $q_{x,i}$ and $q_{y,i}$, so that the x- and y- components of ground speed are $r_{x,i} = q_{x,i} + w_{x,i}$ and $r_{y,i} = q_{y,i} + w_{y,i}$. We denote speeds and directions that can be computed from these by $v_{w,i}$, $v_{q,i}$ and $v_{r,i}$ and by $\vartheta_{w,i}$, $\vartheta_{q,i}$ and $\vartheta_{r,i}$. We further denote by $\vartheta_{w,target,i}$ the angle between the wind and the target, the amount of drift by crosswind by $c_i = v_{w,i}\sin(\vartheta_{w,target,i})$, and the amount of headwind by $h_i = -v_{w,i}\cos(\vartheta_{w,target,i})$. We note that headwind

slows down the advancement toward the target whereas tailwind (negative values of headwind) speeds it up.

We assume that the crane adjusts its air speed by increasing the air speed in case of headwind or decreasing it in case of tailwind (Hedenström and Alerstam 1995; Newton 2010). For simplification reasons we ignore the fact that birds also increase their speed to compensate for drift (Liechti et al. 1994; Liechti 1995), which is modelled by a change in direction. Due to these adjustments, the speed and the direction of the crane are modelled as functions of

$$v_{q,i} = v_q(b_1, b_2, h_i), \ \vartheta_{r,i} = f(a, c_i, v_{q,i}), \tag{3}$$

where b_1 and b_2 are parameters of the *power curve* (Pennycuick 1978) that map the headwind into the crane's air speed.[5] a is a parameter that describes to what extent the crane compensates for drift. Given the fact that air speed $v_{q,i}$ depends on heading $\vartheta_{q,i}$ and vice versa, these variables are determined sequentially in a recurring function, initialised at $v_{q,i} = 18ms^{-1}$ and looped 3 times. After testing this function under various wind conditions it was found that it quickly results in equilibrium values for $\vartheta_{q,i}$ and $v_{q,i}$. Furthermore, in M3 we include a similar adjustment in direction ϑ_i as in M2, based on measured direction ϑ_0 and the temporal autocorrelation in direction

$$\vartheta_i = \vartheta_{r,i} + (\vartheta_0 - \vartheta_{r,i})\gamma_\vartheta^i. \tag{4}$$

The parameter vector θ of this model is $\theta = (a, c_1, c_2, \gamma_\vartheta)$, out of which a is assumed to be different for spring and autumn.

2.3. Parametrisation

2.3.1. Speed

Ground speed v_μ in M1 and M2 is parametrised based on ground displacement and time interval between subsequent GPS fixes, by taking the mean ground speed in the training data set of GPS fixes. Temporal autocorrelation in flight speed γ_v in M2 is determined by the Pearson correlation coefficient between ground speed measured at i and ground speed measured at $i+1$.

The coefficients c_1 and c_2 that determine air speed in M3 are derived from the relationship between inferred air speed v_r and the amount of headwind h. We assume that cranes maximise their range (relative to ground) per unit energy (Pennycuick 1978). Hence, we parametrise the model describing the relationship between air speed and head wind (or tail wind) with a function that assumes maximum range speed.[6] We denote δ as

$$\delta = (v_q(b_1, b_2, h_i) - h)^2 + h^2, \tag{5}$$

where b_1 and b_2 are the regression coefficients of a linear regression with

---

[5] In our study we assume a simplified quadratic function of the power curve, i.e., the power needed for flight increases quadratically with air speed. This fits with the assumption that the power curve is U-shaped, although we acknowledge that air resistance is in fact a cubic function of speed according to the laws of aerodynamics (Liechti 1995, Rayner 1999) and that the power curve is not necessarily u-shaped (Rayner 1999). However, after experimenting with various hypothetical power curves we concluded that the quadratic approximation works particularly well in the domain between the minimum power required for flight (vq at minimal metabolic power) and the maximum range speed for $vw = 0$. This reflects the domain of tailwinds and correspondingly the air speeds at which cranes are predominantly flying. Moreover, it is much easier to find an analytical solution for the relationship between vq and vw when we assume the power curve is parabolic.

[6] We acknowledge that migratory birds could adopt different strategies in flight speed, e.g. minimizing migration time or minimizing energy expenditure. However, distinguishing between flight speed that maximises range or minimises migration time will be quite challenging in practice as the difference are expected to be small (Alerstam & Hedenström 1998).

Table 2
Key features of the different models used in our analysis.

Models Features	M1 (benchmark)	M2	M3
Speed autocorrelation	–	X	–
Direction autocorrelation	–	X	X
Wind data	–	–	X
Drift	Not applicable	Not applicable	0 %, 10 %, 20 %, 30 %

δ as dependent variable and h as independent variable, fitted on training data. Modelled air speed $v_{q,i}$ is then determined by

$$v_{q,i} = \sqrt{b_1 + b_2 * h + h^2} + h. \tag{6}$$

2.3.2. Heading

Temporal autocorrelation in flight direction, γ_ϑ in M2 and M3, is parametrised in a similar way as autocorrelation in flight speed. We first determine the difference between measured flight direction $\vartheta_{r,i}$ and target direction $\vartheta_{target,i}$ for all subsequent GPS fixes in the training data, and then assess the correlation between the difference measured at i and the difference measured at $i + 1$ using a circular version of the Pearson correlation coefficient (Jammalamadaka and Sarma 1988). We assume that γ_ϑ is the same for M2 and M3, as the individual variation in track direction is much larger than the variation in wind direction along the route.

In M3, we determine a by the degree cranes adjust their heading in order to compensate for wind drift. If and to what extent they do so is represented by three possible strategies illustrated in Appendix I: full drift, full compensation and partial compensation/partial drift. In case of full drift ($a = 1$) then crane heading ϑ_q equals ϑ_{target}, and track direction ϑ_r equals ϑ_{target} in case of full compensation ($a = 0$). We determine a by denoting α as the angle between ϑ_q and ϑ_r, and plotting ϑ_q and ϑ_r against α under various wind conditions. Based on Green and Alerstam (2002) we estimate the regression coefficient between α and ϑ_r, and between α and ϑ_q in order to establish the amount of drift and compensation respectively. a is directly represented by the coefficient for ϑ_r as function of α, which ranges between 0 for full compensation and 1 for full drift. Whereas a can also be found by $a - 1$; the coefficient for ϑ_q as function of α, which ranges between -1 for full compensation and 0 for full drift. We use method 1 in Green and Alerstam (2002), where we aggregate the mean of ϑ_q and ϑ_r for 36×10-degree bins of wind directions ϑ_w. For comparison, we also apply a disaggregated method based on the same principles but in this case we plot $\vartheta_{q,target}$ and $\vartheta_{r,target}$, defined respectively as direction and heading relative to the target, against α. This allows us to estimate the regression coefficients based on all individual GPS fixes in the training data. Note that this method can only be applied when the target is known, which is the case for the cranes in our study area.

2.4. Cross-validation

To validate each model's forecasting performance under various forecasting ranges, we run a cross-validation experiment using various time lags ranging from fifteen minutes up to four hours and fifteen minutes. We used lag 2, 3, 4, 5, 6, 8, 10, 12, 15, and 18, indicating the number of GPS fixes (with a fifteen-minute interval) that were included in each forecast. Lag 2 indicates 2 GPS fixes and a forecasting range of 15 min, lag 18 indicates 18 GPS fixes and a forecasting range of 255 min, etcetera. The first GPS fix was used as a starting point for each forecast, and the comparison (predicted minus observed) was made only with the last GPS fix, comparing the angle and speed between the first and the last observation/prediction using the shortest geodesic distance between these points.

We selected unique combinations of crane individuals and migration days (henceforth: individual migration events) over our study area. This yields 42 individual migration events during spring migration (February-March) and 51 individual migration events during autumn migration (October-November). Of each individual migration event we selected GPS fixes classified as *flying* (Section 2.1.1), and split them into *N/lag* subsets, where N represents the number of GPS fixes in each individual migration event. Forecasts were done for all subsets that fitted in a lag, using discrete steps corresponding with the time intervals between GPS fixes in the subsets. Table 3 presents a summary of the experiment.

Table 3

Summary of the number of forecast steps, forecasting range, and number of subsets (= number of forecasts) per lag.

Lag	Number of steps in forecast	Forecasting range (minutes)	Number of subsets autumn	Number of subsets spring
2	1	15	440	430
3	2	30	326	274
4	3	45	213	214
5	4	60	219	168
6	5	75	163	131
8	7	105	131	89
10	9	135	78	68
12	11	165	62	49
15	14	210	48	36
18	17	255	32	25

We perform leave-one-out cross validation, where the training data to parametrise models 1–3 excluded the migration events corresponding to the respective subsets. We used root mean squared error (RMSE) and prediction bias for both flight speed and direction as performance metrics to evaluate the three models' forecasting performance.

In defining the parameter space for a in M3, we must note that finding the exact amount of drift is not trivial (Green and Alerstam 2002). We therefore test M3 several times with multiple values of drift: 0 %, 10 %, 20 %, and 30 %. For 0 % drift it is easy to determine α. However, for any amount of drift higher than 0 % and lower than 100 % (i.e., in case of partial drift and partial compensation), there is no analytical solution for α. Hence, α must be estimated by careful weighing of equation A1 and equation A2 (Appendix I) depending on ratio between c_i, $v_{q,i}$ and h_i, and the amount of drift a. We decided to simplify the calculation of α so that it resembles that of full compensation (equation A2 in Appendix I) because: (1) compensation has the upper hand in our model parameters as well as in our analysis of GPS data (0–30 % drift, 70–100 % compensation); (2) the majority of the measured values of α are between $-63°$ and $+63°$ (yielding relatively marginal differences between the sin and tangent of α), and (3) cranes are typically found to restrict their migration to favourable wind conditions that allow little drift (see results Section 3.1). We believe that this simplification for finding α is justifiable since any forecasting errors produced by uncertainties about the ecological process of migration are several orders of magnitude larger than any errors caused by mathematical imprecisions.

3. Results

3.1. Speed

3.1.1. GPS analysis

The average flight speed (v in M1 and v_μ in M2) of the cranes differed by 0.3m s^{-1} between spring and autumn. Mean ground speed was 14.3m s^{-1} during spring migration and 14.6m s^{-1} during autumn migration, with standard deviations of 5.8m s^{-1} and 4.3m s^{-1} respectively in spring and autumn. The correlation coefficient measuring temporal autocorrelation in flight speed, γ_v in M2, was high: 0.79. This indicates that ground speed is rather persistent per individual migration event.

In M3 we established the contribution of wind on ground speed per migration event. Here, cranes are found to adjust their air speed depending on the strength of headwinds or tailwinds; they fly slower in tailwinds and faster in headwinds. Fig. 2 shows a continuous increase in airspeed as a function of headwind, which accelerates when headwinds become stronger. In this domain it makes sense to spend more energy by flying faster to achieve maximum range relative to the energy spent on flying against the wind (Newton 2010). In the opposite domain birds can take advantage of tailwinds by flying slower and conserving energy. However, there is a limit to how slow birds can fly, otherwise they would require more power to generate enough lift to remain airborne. This
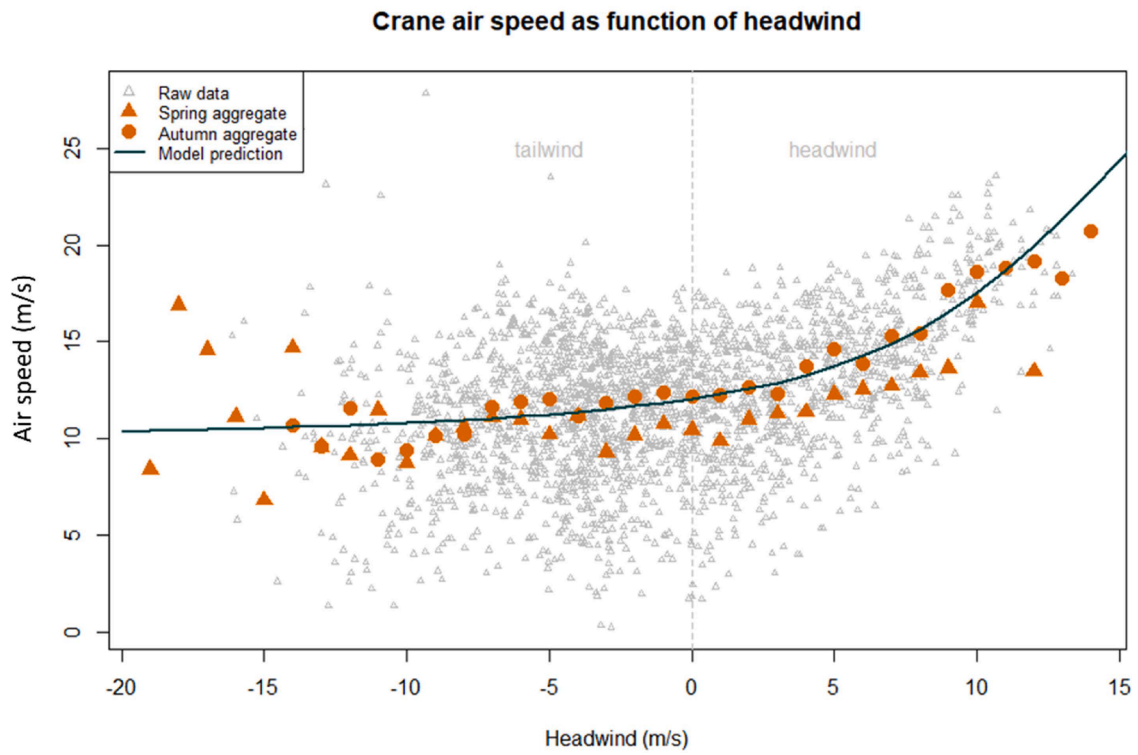
Crane air speed as function of headwind

Fig. 2. Crane air speed as function of tailwind/headwind with a model prediction (line) based on the 'power curve' in Pennycuick (1978). Raw data is shown in grey and orange dots indicate the mean air velocity for 1ms^{-1} bins of headwind during spring migration (triangles) and autumn migration (circles).
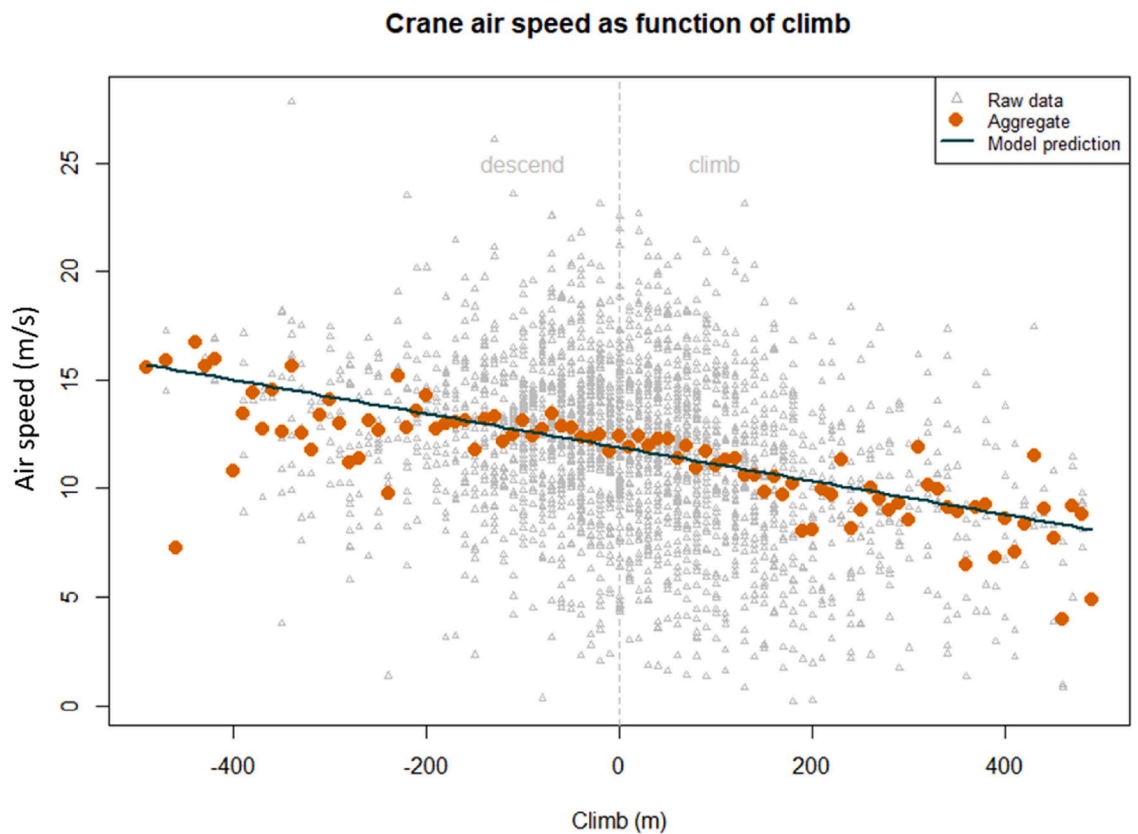
Crane air speed as function of climb

Fig. 3. Crane air speed as a function of descend/climb. Line indicates model predictions based on linear regression.

relationship is described by the 'power curve' in Pennycuick (1978), which shows the relationship between a bird's air speed and the power needed for flight. The power curve can be used to hypothesise an optimum flight speed where the flight range is maximised and the total metabolic cost is minimised. Fig. 2 illustrates predictions of where this optimum lies based on the cranes' GPS data. Particularly noticeable is the fact that cranes only seem to follow this predicted optimum during autumn migration, whereas they fly considerably slower than the predicted optimum in spring. On average they fly 1.2 metres per second below the predicted optimum, which is approximately 10 % slower than expected.

Air speed is also affected by climbing/descending (Fig. 3), whereby air speed decreases with altitude gain and increases with altitude loss. It seems that the relationship is not exactly linear, as there seems to be a negative prediction bias in the centre of the climbing/descending range and a positive prediction bias towards both extremes.

3.1.2. Model forecast

The RMSEs of M2 and M3 in predicted ground speed are much lower than M1 (Fig. 4, left panel). In M1 and M2 there is also a distinct difference in RMSE values between seasons; the prediction error of speed is generally larger in spring than in autumn, indicating that flight speed in spring has more variance which is unaccounted for in M1 and M2. M3 on the other hand has little differences in RMSE values between spring and autumn. It seems that by including wind data, M3 accounts for the larger variance in flight speed in spring.

In terms of RMSE values over time, we see that M2 has the lowest RMSE in the short forecast range (<1 hour). This makes sense, since this model uses information of flight speed at t, and there is a strong autocorrelation in flight speed between t and $t + 1$ hour. In the longer forecasting range (>1 hour) M3 outperforms M2. Where RMSE values in M1 and M2 are fairly constant over different forecast ranges, RMSE values in M3 gradually decrease with increasing forecasting range. Hence, the inclusion of wind data in M3 improves the forecast horizon of

flight speed in comparison to both M1 and M2. The result that RMSE decreases may seem contradictory to the general principle that forecasting errors increase with increasing forecasting range. This principle holds when we would look at RMSE of absolute distance travelled. Yet, the total variance in (observed and predicted) flight speed actually decreases because it is averaged over a longer time spent flying.

In terms of prediction bias, the most notable result is the positive bias in flight speed in M3 in spring (Fig. 4, right panel). This shows how our observation, that cranes are flying much slower than expected in spring (Section 3.1.1), propagates into forecasts that are biased by more than five kilometres per hour. We found that this bias is resolved when the M3 is trained separately for each season (see: Appendix III). Furthermore, where RMSE values of M3 seems to be independent of the drift parameter, model bias seems to be more sensitive to the amount of drift: the prediction bias of M3 tends to be more positive with higher amounts of drift. This can be explained by the fact that cranes will achieve a further range when they accept more drift. Hence, a trade-off may exist between compensating for drift to stay on track or allowing some drift to cover more distance and getting closer to target (Liechti 1995).

3.2. Heading

3.2.1. GPS analysis

Temporal autocorrelation in track direction with respect to the target, γ_ϑ in M2, was lower than temporal autocorrelation of flight speed: 0.62. This indicates that there is indeed some directional persistence in flight direction when looking at tracks of individual migration events. Yet, there is also randomness in that cranes change their direction regularly between the 15-minute time intervals, making it hard to forecast their direction for hours in advance.

Estimating the amount of drift in M3 based on GPS data proves to be a challenging topic, yielding inconsistent results depending on the chosen method (Fig. 5). The Green and Alerstam method to analyse drift on aggregated data (Fig. 5, left panels) shows that cranes experience 15
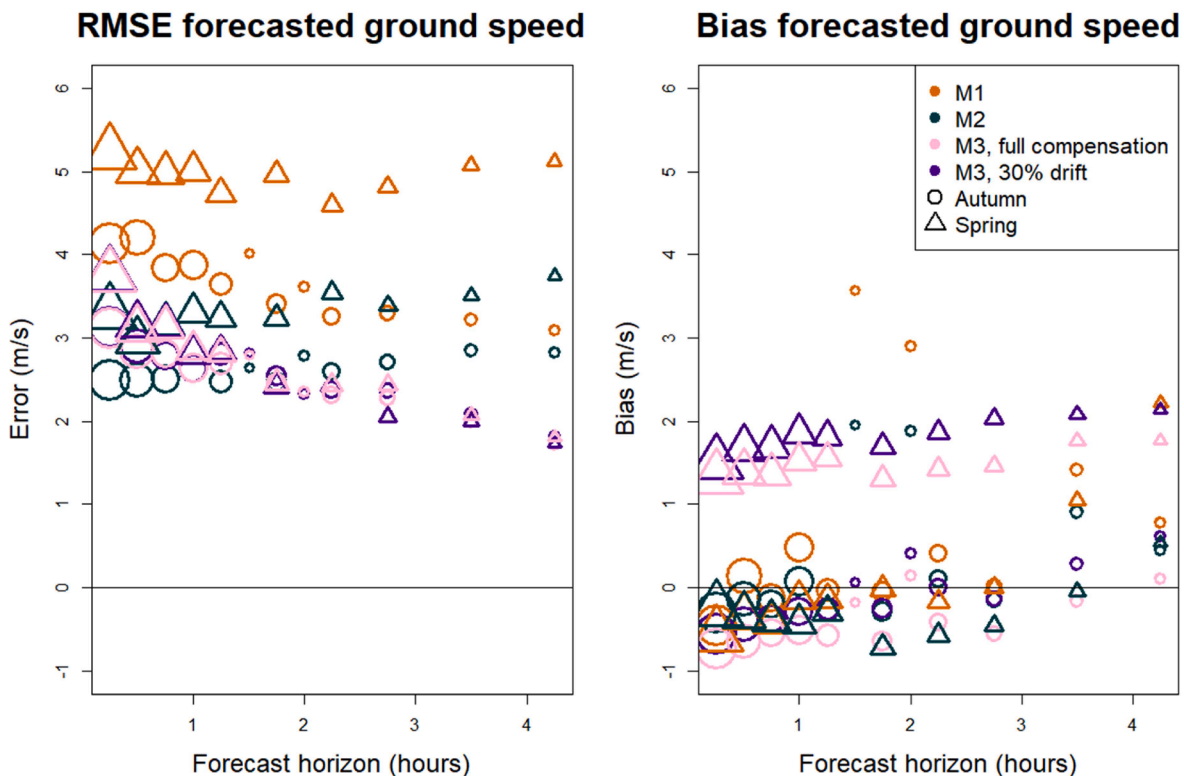

Fig. 4. Performance of models 1–3 in predicting ground speed over time during spring and autumn migration. The panel on the left shows root mean squared error (RMSE) and the panel on the right shows the prediction bias. Shapes vary in size according to number of observations – larger shapes represent more observations.
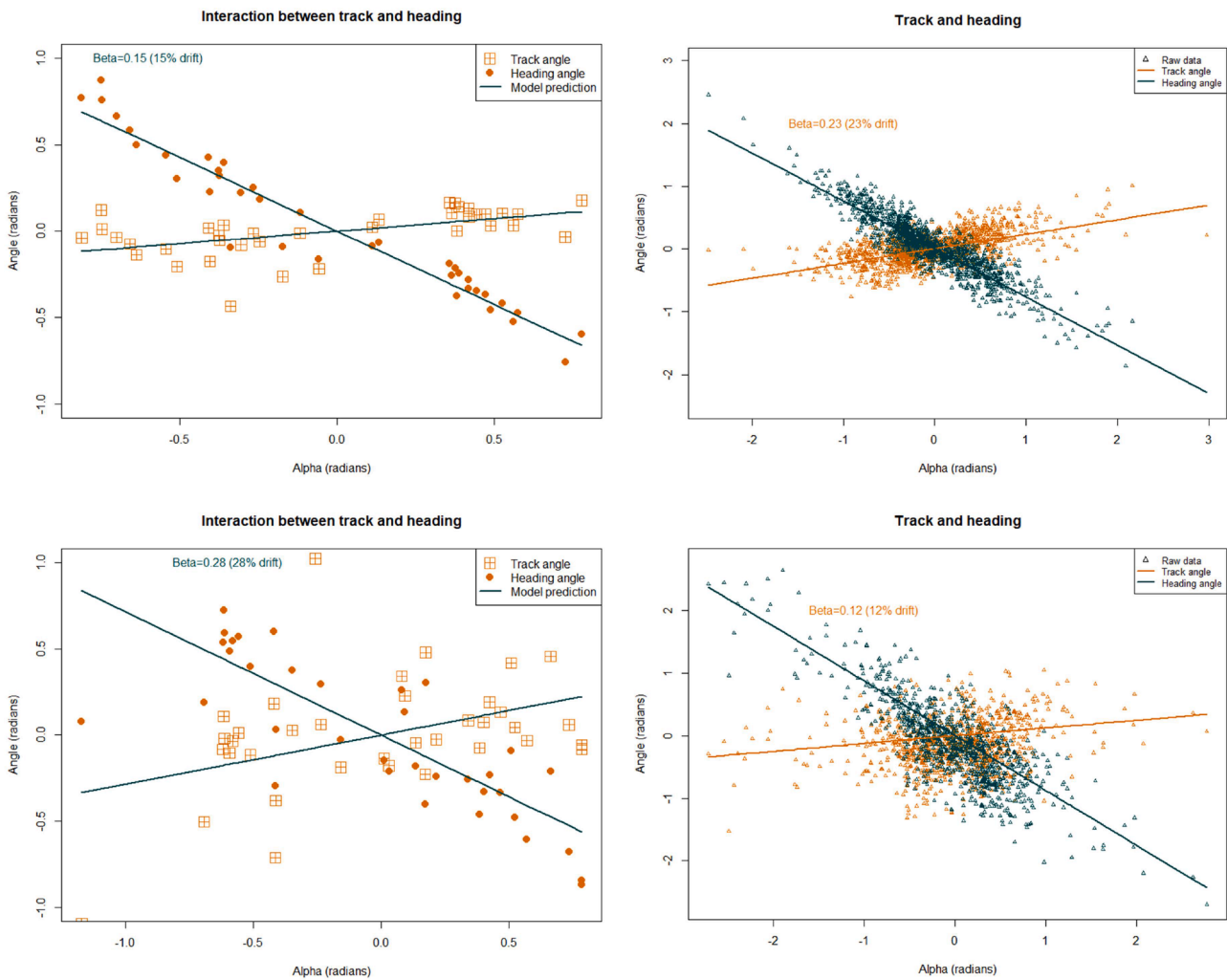
Fig. 5. The relationship between track and heading used for estimating the amount of drift in autumn (top panels) and spring (bottom panels). The left panels show estimated drift with aggregated data based on the proposed method of Green and Alerstam (2002), whereas the right panels show estimated drift with disaggregated data and a presumably known target location.

% drift during autumn migration and 28 % during spring migration, which is considerably more in spring. However, on the disaggregated data with a presumably known target destination (Fig. 5, right panels) we find that cranes drift much more during autumn migration than during spring migration (23 % versus 12 % respectively).

It also seems that there is much more uncertainty in the estimated amount of drift in spring than in autumn, indicated by a much bigger spread in track and heading angles in spring (Fig. 5, bottom panels). The two estimates yielded by the different methods are also further apart in spring than in autumn. Nonetheless, with a share of at least 72 % and at most 88 % according to our results, compensation has a much bigger share of a crane's migration strategy than drift (at least 12 % and at most 28 %), both in autumn and in spring.

3.2.2. Model forecast

Looking at the performance of our models in predicting flight heading, a few things stand out. Firstly, the differences in RMSE values between the three models are largest in the shorter forecasting range (<2 h), in particular because M1 has very high RMSE values. These values steadily decline as forecasting range increases (Fig. 6, left panel). The fact that RMSE declines with increasing forecasting range can primarily be attributed to the fact that the variance in track direction decreases with increasing flight distance, similar to what we saw in RMSE of flight speed. In the short time span the flight direction of cranes is

much more variable, which is not accounted for in the forecasts of M1, whereas it is accounted for in the forecasts of M2 and M3. M2 and M3 have much lower RMSE values in the shorter forecast range since forecasts are based on flight headings observed at t and temporal autocorrelation between heading at t and heading at $t + \Delta t$. Secondly, RMSE values are consistently higher in spring than in autumn in all models, indicating that flight heading is a lot more unpredictable in spring than in autumn. Thirdly, M2 and M3 hardly differ in prediction performance in particular in spring, which suggests that adding wind data does not contribute much to forecasting cranes' flight heading. This makes sense in case of full compensation, as cranes are then supposed to fly straight towards their intended target, same as in M2 that excludes wind data. When the amount of drift in M3 increases, we do see that it reduces the RMSE in particular in autumn, which suggests that part of the variance in flight heading in autumn can indeed be explained by wind drift.

Lastly, we see that there is a consistent negative bias in forecasted heading in spring in all models (Fig. 6, right panel). A negative prediction bias means that the observed flight directions are more towards the right of the predicted flight directions. This bias may be caused by the fact that the model assumes only a single possible migration route via Bremen-Hemelsmoor-Hamburg to cross the Baltic Sea at Rügen. Whereas our GPS dataset also contains cranes with a more southeasterly route via Frankfurt and Magdeburg.
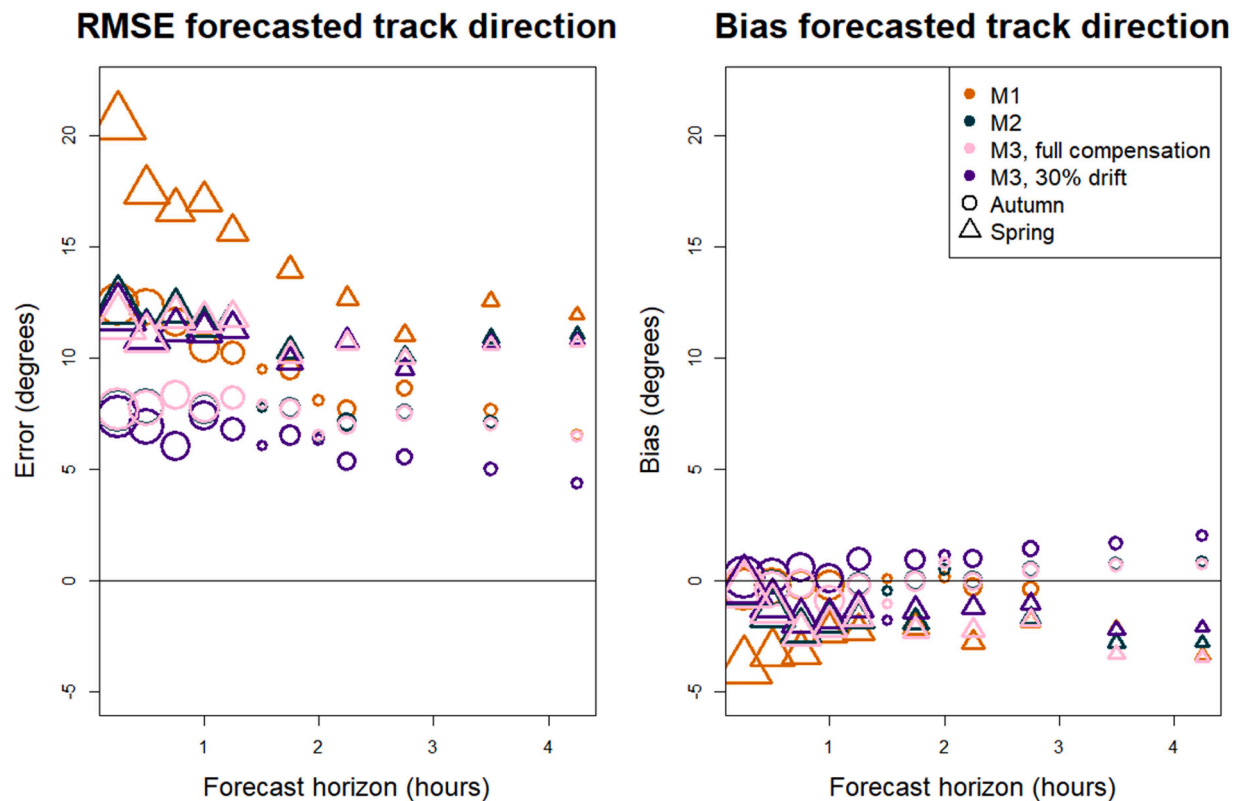
RMSE forecasted track direction

Bias forecasted track direction

Fig. 6. performance of models 1–3 in predicting flight direction over time during spring and autumn migration. The panel on the left shows root mean squared error (RMSE) and the panel on the right shows the prediction bias. Shapes vary in size according to number of observations – larger shapes represent more observations.

4. Discussion

4.1. Factors that improve predictions

In this paper we explored the performance of three different models forecasting the speed and direction of cranes migrating over the Benelux, western Germany and northern France. The observation data required to parametrise these models varied between GPS fixes only (M1 and M2), and a combination of GPS fixes and ERA5 reanalysis data of wind at 950hPa and 975hPa (M3). Furthermore, all three models assume a known target direction in spring (Hemelsmoor, Germany) and autumn (Lac du Der, France). Once parameterised, M1 needs a latitude, a longitude and a timestamp of a flock of cranes in order to forecast their migration route. M2 additionally needs an observation of speed relative to the ground, and of flying direction relative to the target. M3 needs the same as M1, and additionally an observation of flying direction and a forecast of wind speed and direction at flying altitude (e.g., at the 950hPa pressure level).

4.1.1. Observations of speed and direction

Our results show that M2 predicts flight speed and direction much better than M1, particularly in the first hours of the forecasts. As expected, the performance metrics of M1 and M2 tend to converge with a longer forecasting horizon, since the autocorrelation in speed is negligible after two hours. In other words, the inclusion of temporal autocorrelation benefits the short-range forecasts of the crane migration. However, it does require measurements of flight direction and speed. Acquiring these estimates from ground observations, e.g., citizen science data from birdwatchers, is fairly easy for flight direction. Yet, reliable speed estimates require much more laborious approaches, following individual flocks, or expensive equipment such as radar tracking devices (Bruderer and Steidinger 1972). Moreover, it needs to be considered that speed and heading in our models are based on 15-minute intervals while

field observations will correspond more to instantaneous measurements which add more variance to the observed speed and heading.

4.1.2. Wind forecasts at flight altitude

Comparing M3 with the predictions of M1 and M2, we saw that adding wind data resulted in a more consistent improvements in the forecasts of speed over the entire temporal range. Although in the first hour M2 predicted speed better than M3, the forecasts of M3 improved with respect to the other two models as the forecast range increased. Wind data are thus a valuable addition in forecasting migration over longer time spans. The advantage of wind forecasts (M3) compared to flight speed (M2), is that there are openly accessible wind forecasts at flight altitude available.[7] In terms of flight direction, we however found that adding wind data did not improve the forecasting performance of M3. This is not surprising, since cranes were found to mostly compensate for wind drift and so wind has less impact on flight direction. In fact, compensation for drift was hard-wired in M3 based on these observations. One exception is that M3 was more accurate in autumn when we assumed more drift, particularly in the long forecasting range, whereas in spring such improvement was not found in M3. For birds that drift more during migration, such as juveniles (Thorup et al. 2003; Sergio et al. 2022) or nocturnal migrants (Van Doren et al. 2016), adding wind data might still be a valuable addition to flight direction forecasts.

4.1.3. Altitude changes

Climbing/descending was also an important factor in determining flight speed, but this was not included in our prediction models for two reasons. First, soaring and gliding cycles of cranes are in the order of a few minutes (Pekarsky et al. 2024), whereas the intervals in our GPS data are 15 min. The sections between two fixes therefore cannot be

---

[7] https://dataplatform.knmi.nl/group/weather-forecast

classified into two discrete modes of flight that drive altitude changes. Secondly, for forecasting purposes any observations of past altitude gains/losses would hardly be useful, since the independent variable 'climbing/descending' would have to be forecasted as well. It would only be useful if this variable can be linked with other environmental features that are either fixed or for which a reliable forecast is available. Future work can focus on forecasts for soaring behaviour based on thermal and orographic uplift velocities, derived from weather forecasts and elevation maps (Bohrer et al. 2012; Scacco et al. 2019). Yet, these predictions would then rather address flight speed indirectly through predicted altitude gains and losses depending on the atmospheric conditions for soaring.

4.1.4. Known destination of migration

Another factor that positively affected the forecasting ability was the target destination. Our approach is based on known stopover sites that the cranes are very likely to visit. However, this is not generally the case for migrants, in many cases individuals passing in a specific area do not have a fixed destination as the cranes. However, we think the model can reasonably be generalised for other species by assuming an average migration direction or destination area. The consequences of such a generalisation for the accuracy of the model will vary on a case by case basis and should be evaluated.

4.2. Spring migration more challenging to forecast than autumn migration

In general, we found that spring migration was harder to predict than autumn migration. First of all, there was a consistent bias in flight speed predictions in M3. Despite the overall higher prediction accuracy of M3, we found that cranes flew much slower in spring than M3 predicted. When correcting for wind, cranes flew faster in autumn than in spring. Kemp et al. (2010) found that nocturnal migratory birds in Western Europe migrate faster during spring than autumn, supported by weather patterns that favour migration speed. However, they also found that air speeds were slower in spring than in autumn, consistent with our findings and the hypothesis that birds fly faster in headwinds and slower in tailwind to optimise their energy expenditure rather than migration speed. Yet, this would not explain why the cranes were flying slower than expected under the energy-optimisation hypothesis. Possibly, this seemingly sub-optimal behaviour could be explained by the fact that all of the studied cranes were inexperienced juveniles, still following their parents in autumn whereas they migrate independently during spring (Alonso et al. 1984). Another explanation could be a higher use of thermal soaring due to more favourable thermal conditions in spring compared to autumn, affecting the average air speed (Swanberg 1987; Newton 2010). An F-test on the variance in altitude gains and losses revealed that there is more variance in altitude in spring compared to autumn ($F = 0.67745$, num df $= 1481$, denom df $= 1249$, $p < 0.001$), which hints on more use of thermal soaring in spring if we assume altitude variations in our GPS data are reliable proxy for soaring behaviour.

Secondly, all models had a higher RMSE in flight direction forecasts in spring compared to autumn. We believe that this is mostly due to the fact that flight directions varied more in spring. This could again be explained by the cranes' inexperience, but also by differences in destinations. Where cranes consistently targeted Lac-du-Der in autumn, in spring they follow various routes towards and across the Baltic Sea, leading to incorrect assumptions in the models about the cranes' target direction. To make our models more flexible on the assumed target direction, Bayesian state-space models could be used in the future (Pirotta et al. 2018). However, such models would require more sophisticated observation approaches, tracking individual flocks for an extended period of time.

4.3. Mixed flight modes by cranes may complicate migration optimization

It is noteworthy to mention that optimality assumptions of adjustments in flight heading and speed, as modelled by Liechti (1995) and Alerstam (1979), are based on powered flights (i.e., wing flapping). Cranes and other soaring migrants have an additional strategy that these models do not account for which may add complexity to migration optimization, namely the use of thermals to gain altitude and generate more potential energy. It has been shown that, by combining soaring, gliding and powered flights, cranes are highly variable in their flight speed, and optimal flight speeds are seldom maintained for long (Pennycuick et al. 1979). These observations suggest that the variance in flight speed and direction of our cranes may have been caused by behavioural changes during migration which our models did not account for. The great variance of environmental conditions along the route make it difficult to fit flight metrics into any of the theoretically optimal behaviours (Hedenström and Alerstam 1995). In other words: even with well-parameterised mechanistic models describing optimal flight strategies, based on power curves and glide polars, there is a limit to the forecastability of migration patterns. Limited by the resolution and accuracy of weather forecasts and by random variations in the behaviour of the cranes. Local variability and low predictability in weather conditions pose a demand on cranes to be flexible in adjusting their flight strategy during migration when conditions change along the route. The question remains whether adding complexity to the models presented here would improve forecasting performance, as it would also require more complexity in environmental data, forecasts of additional weather metrics in combination with optimisation models addressing various flight modes.

5. Conclusion

In this study we demonstrated the accuracy of models forecasting bird migration, with a focus on single species and even individual flocks instead of large-scale bird migration patterns that are already addressed in radar studies (Van Doren and Horton 2018; Horton et al. 2021; Kranstauber et al. 2022). The models presented here are flexible in that they can combine ground observations, for example using citizen-science based observations from birdwatchers, with other data such as GPS telemetry. Another unique aspect about our study is that we quantitatively assessed the prediction performances over different forecast ranges, thereby providing an actual test of the models' forecasting capabilities. These kind of analyses shed light on the performance limits of forecast models, which has important implications for model-based decision making in ecology.

Our analysis illustrates that weather forecast models significantly can improve the forecast horizon for predicting the migration routes of individual flocks of birds. At the same time we shed light on the remaining variance that our models cannot address (yet). Eliminating the remaining uncertainty opens new avenues for fundamental research in migration ecology. We conclude that the uncertainty in flight speed (RMSE between 2.5 m s^{-1} and 5.0 m s^{-1}) is larger than the uncertainty in flight direction (RMSE between 7 and 17°, corresponding to 1.7–4.2m s^{-1} drift from the expected flight direction). Yet, we also argue that the uncertainty in direction is more problematic than the uncertainty in speed in the majority of applications. Errors in the forecasted flight speed impact the estimated timing of arrival on a particular site, whereas errors in direction impacts our estimation of the location and routes where cranes will pass. In the proposed applications of our models, errors in direction forecasts imply directing birdwatchers to the wrong locations or worse: stopping the wrong wind turbines. Leading to economic losses and possibly still risking deadly collisions. Speed forecasts on the other hand only affect the time window of the expected likelihood of collisions. Hence, we stress that flight direction should be a standard metric to record in order to facilitate migration forecasts, particularly in the short range. For longer forecast horizons, our models

could benefit from a better understanding of the factors that determine the variance in flight direction, apart from wind drift and target destination. Further research in migration ecology should therefore investigate what drives cranes, and other migratory birds, to fly in certain directions and to follow certain migration routes.

CRediT authorship contribution statement

K. De Koning: Writing – original draft, Visualization, Validation, Methodology, Investigation, Formal analysis. **L. Nilsson:** Writing – original draft, Resources, Data curation. **J. Månsson:** Writing – original draft, Resources, Data curation. **O. Ovaskainen:** Writing – original draft. **B. Kranstauber:** Writing – original draft. **M. Arp:** Validation, Software, Data curation. **J.K. Schakel:** Funding acquisition.

Declaration of competing interest

The authors declare that they have no known competing financial interests or personal relationships that could have appeared to influence the work reported in this paper.

Acknowledgement/Funding

Supplementary materials

Supplementary material associated with this article can be found, in the online version, at doi:10.1016/j.ecolmodel.2024.110884.

Data availability

Data will be made available on request.

References

Alerstam, T., 1979. Wind as selective agent in bird migration. Ornis Scandinavica 76–93.
Alerstam, T., Hedenström, A., 1998. The development of bird migration theory. J. Avian Biol. 343–369.
Alonso, J.C., Veiga, J.P., Alonso, J.A., 1984. Family breakup and spring departure from winter quarters in the common crane Grus grus. J. für Ornithologie 125, 69–74.
Arts, K., Van der Wal, R., Adams, W.M., 2015. Digital technology and the conservation of nature. Ambio 44, 661–673.
Aurbach, A., Schmid, B., Liechti, F., Chokani, N., Abhari, R., 2018. Complex behaviour in complex terrain-modelling bird migration in a high resolution wind field across mountainous terrain to simulate observed patterns. J. Theor. Biol. 454, 126–138.
Bohrer, G., Brandes, D., Mandel, J.T., Bildstein, K.L., Miller, T.A., Lanzone, M., Tremblay, J.A., 2012. Estimating updraft velocity components over large spatial scales: contrasting migration strategies of golden eagles and turkey vultures. Ecol. Lett. 15 (2), 96–103.
Bouten, W., van Belle, J., van Gasteren, H., Vrugt, J.A., Shamoun-Baranes, J., Buurma, L., 2005. Predicting bird migration: data-driven versus concept-driven models. In: Proceedings of the 27th International Bird Strike Committee Meeting, pp. 19–31.
Bradarić, M. (2022). On the radar: weather, bird migration and aeroconservation over the North Sea.
Bruderer, B., & Steidinger, P. (1972). Methods of Quantitative and Qualitative Analysis of Bird Migration with a Tracking Radar. NASA, Washington Animal Orientation and Navigation.
Bulte, M., McLaren, J.D., Bairlein, F., Bouten, W., Schmaljohann, H., Shamoun-Baranes, J., 2014. Can wheatears weather the Atlantic? Modeling nonstop trans-Atlantic flights of a small migratory songbird. Auk: Ornithol. Adv. 131 (3), 363–370.
Clark, J.S., Carpenter, S.R., Barber, M., Collins, S., Dobson, A., Foley, J.A., Wear, D., 2001. Ecological forecasts: an emerging imperative. Science (1979) 293 (5530), 657–660.
de Koning, K., Broekhuijsen, J., Kühn, I., Ovaskainen, O., Taubert, F., Endresen, D., Grimm, V., 2023. Digital twins: dynamic model-data fusion for ecology. Trends Ecol. Evol. (Amst.).
De Lucas, M., Ferrer, M., Bechard, M.J., Muñoz, A.R., 2012. Griffon vulture mortality at wind farms in southern Spain: distribution of fatalities and active mitigation measures. Biol. Conserv. 147 (1), 184–189.
Dietze, M.C., Fox, A., Beck-Johnson, L.M., Betancourt, J.L., Hooten, M.B., Jarnevich, C.S., White, E.P., 2018. Iterative near-term ecological forecasting: needs, opportunities, and challenges. Proc. Natl. Acad. Sci. 115 (7), 1424–1432.
Duriez, O., Bauer, S., Destin, A., Madsen, J., Nolet, B.A., Stillman, R.A., Klaassen, M., 2009. What decision rules might pink-footed geese use to depart on migration? An individual-based model. Behav. Ecol. 20 (3), 560–569.
Fischer Jr, R.A., Guilfoyle, M.P., Valente, J.J., Gauthreaux, S.A., Belser, C.G., Van Blaricom, D., … & Moore, F.R. (2012). The identification of military installations as important migratory bird stopover sites and the development of bird migration forecast models: a radar ornithology approach.
Green, M., Alerstam, T., 2002. The problem of estimating wind drift in migrating birds. J. Theor. Biol. 218 (4), 485–496.
Hedenström, A., Alerstam, T., 1995. Optimal flight speed of birds. Philos. Trans. R. Soc. Lond. Ser. B: Biol. Sci 348 (1326), 471–487.
Hersbach, H., Bell, B., Berrisford, P., Biavati, G., Horányi, A., Muñoz Sabater, J., Nicolas, J., Peubey, C., Radu, R., Rozum, I., Schepers, D., Simmons, A., Soci, C., Dee, D., Thépaut, J.-N., 2023. ERA5 hourly data on pressure levels from 1940 to present. Copernicus Climate Change Serv. (C3S) Climate Data Store (CDS). https://doi.org/10.24381/cds.bd0915c6 (Accessed on 08-04-2022).
Holleman, I., 2008. Wind observations with Doppler weather radar. In: TECO-2008—WMO Technical Conference on Meteorological and Environmental Instruments and Methods of Observation. St. Petersburg, Russian Federation, 27–29 November 2008.
Horton, K.G., Van Doren, B.M., Albers, H.J., Farnsworth, A., Sheldon, D., 2021. Near-term ecological forecasting for dynamic aeroconservation of migratory birds. Conservat. Biol. 35 (6), 1777–1786.
Jammalamadaka, S.R., Sarma, Y.R., 1988. A correlation coefficient for angular variables. Stat. Theory Data Anal. II 349–364.
Keitt, T.H., Abelson, E.S., 2021. Ecology in the age of automation. Science (1979) 373, 858–859.
Kemp, M.U., Shamoun-Baranes, J., Van Gasteren, H., Bouten, W., Van Loon, E.E., 2010. Can wind help explain seasonal differences in avian migration speed? J. Avian Biol. 41 (6), 672–677.
Kranstauber, B., Bouten, W., van Gasteren, H., Shamoun-Baranes, J., 2022. Ensemble predictions are essential for accurate bird migration forecasts for conservation and flight safety. Ecol. Solut. Evid. 3 (3), e12158.
Lewis, A.S., Rollinson, C.R., Allyn, A.J., Ashander, J., Brodie, S., Brookson, C.B., Wardle, G.M., 2023. The power of forecasts to advance ecological theory. Methods Ecol. Evol. 14 (3), 746–756.
Liechti, F., 1995. Modelling optimal heading and airspeed of migrating birds in relation to energy expenditure and wind influence. J. Avian Biol. 330–336.
Lippert, F., Kranstauber, B., Forré, P.D., van Loon, E.E., 2022. Learning to predict spatiotemporal movement dynamics from weather radar networks. Methods Ecol. Evol. 13 (12), 2811–2826.
Månsson, J., Nilsson, L., Hake, M., 2013. Territory size and habitat selection of breeding Common Cranes (Grus grus) in a boreal landscape. Ornis Fennica 90 (2), 65.
McLaren, J.D., Shamoun-Baranes, J., Bouten, W., 2012. Wind selectivity and partial compensation for wind drift among nocturnally migrating passerines. Behav. Ecol. 23 (5), 1089–1101.
Metz, I.C., Ellerbroek, J., Mühlhausen, T., Kügler, D., Hoekstra, J.M., 2020. The bird strike challenge. Aerospace 7 (3), 26.
Michelot, T., Langrock, R., Patterson, T.A., 2016. moveHMM: an R package for the statistical modelling of animal movement data using hidden Markov models. Methods Ecol. Evol. 7 (11), 1308–1315.
Newton, I., 2010. The Migration Ecology of Birds. Elsevier.
Oloo, F., Safi, K., Aryal, J., 2018. Predicting migratory corridors of white storks, ciconia ciconia, to enhance sustainable wind energy planning: a data-driven agent-based model. Sustainability. 10 (5), 1470.
Pekarsky, S., Shohami, D., Horvitz, N., Bowie, R.C., Kamath, P.L., Markin, Y., Nathan, R., 2024. Cranes soar on thermal updrafts behind cold fronts as they migrate across the sea. Proc. R. Soc. B 291 (2015), 20231243.
Pennycuick, C.J., 1978. Fifteen testable predictions about bird flight. Oikos. 165–176.
Pennycuick, C.J., Alerstam, T., Larsson, B., 1979. Soaring migration of the common crane Grus grus observed by radar and from an aircraft. Ornis Scandinavica 241–251.
Pirotta, E., Katzner, T., Miller, T.A., Duerr, A.E., Braham, M.A., New, L., 2018. State-space modelling of the flight behaviour of a soaring bird provides new insights to migratory strategies. Funct. Ecol. 32 (9), 2205–2215.
Randon, M., Dowd, M., Joy, R., 2022. A real-time data assimilative forecasting system for animal tracking. Ecology. 103 (8), e3718.

Rayner, J.M., 1999. Estimating power curves of flying vertebrates. J. Exp. Biol. 202 (23), 3449–3461.

Ruhe, W., 2008. Bird hazard management in the German armed forces. In: 28th IBSC Conference. International Bird Strike Committee.

Scacco, M., Flack, A., Duriez, O., Wikelski, M., Safi, K., 2019. Static landscape features predict uplift locations for soaring birds across Europe. R Soc. Open Sci. 6 (1), 181440.

Sergio, F., Barbosa, J.M., Tanferna, A., Silva, R., Blas, J., Hiraldo, F., 2022. Compensation for wind drift during raptor migration improves with age through mortality selection. Nat. Ecol. Evol. 6 (7), 989–997.

Swanberg, P.O., 1987. Studies on the influence of weather on migrating cranes (Grus grus) in Sweden. Aquila 93 (94), 203–212.

Thorup, K., Alerstam, T., Hake, M., Kjellén, N., 2003. Bird orientation: compensation for wind drift in migrating raptors is age dependent. Proc. R. Soc. Lond. Ser. B: Biol. Sci. 270 (suppl_1), S8–S11.

Van Belle, J., Shamoun-Baranes, J., Van Loon, E., Bouten, W., 2007. An operational model predicting autumn bird migration intensities for flight safety. J. Appl. Ecol. 44 (4), 864–874.

van der Wal, R., Arts, K., 2015. Digital conservation: an introduction. Ambio 44, 517–521.

Van Doren, B.M., Horton, K.G., Stepanian, P.M., Mizrahi, D.S., Farnsworth, A., 2016. Wind drift explains the reoriented morning flights of songbirds. Behav. Ecol. 27 (4), 1122–1131.

Van Doren, B.M., Horton, K.G., 2018. A continental system for forecasting bird migration. Science (1979) 361 (6407), 1115–1118.

van Gasteren, H., Krijgsveld, K.L., Klauke, N., Leshem, Y., Metz, I.C., Skakuj, M., Shamoun-Baranes, J., 2019. Aeroecology meets aviation safety: early warning systems in Europe and the Middle East prevent collisions between birds and aircraft. Ecography. 42 (5), 899–911.

Van Loon, E.E., Shamoun-Baranes, J., Bouten, W., Davis, S.L., 2011. Understanding soaring bird migration through interactions and decisions at the individual level. J. Theor. Biol. 270 (1), 112–126.